THE AMERICAN SOCIETY OF MECHANICAL ENGINEERS
345 E. 47th St., New York, N.Y. 10017

95-GT-453

RESONANT RESPONSE OF A TAPERED BEAM AND ITS IMPLICATIONS TO BLADE VIBRATION

G. N. Balaji
Department of Mechanical Engineering
Carnegie Mellon University
Pittsburgh, Pennsylvania

J. H. Griffin
Department of Mechanical Engineering
Carnegie Mellon University
Pittsburgh, Pennsylvania

ABSTRACT

The resonant response characteristics of a tapered beam are studied using Euler-Bernoulli beam theory. The sensitivity of the beam's maximum stress to variations in its geometry is studied for three types of harmonic pressure loading. The implications to the response of airfoil chord-wise bending modes are discussed.

1. INTRODUCTION

In 1990 six American gas turbine manufacturers participated in a workshop at Carnegie Mellon University in which they ranked the relative importance of various types of blade vibration problems. They concluded that the fatigue failure of airfoils due to high frequency *tip modes* was their single most important structural problem. Tip modes, which include chord-wise bending modes, are modes in which the displacement at either the leading or trailing edge blade tip is accentuated. Modern blading is more likely to fail from high vibratory response in these types of modes because of the design trend towards wider chords and fewer blades. The use of wider chord vanes and blades tends to make the excitation more severe and make the blade's tip modes more likely to respond. Larger vanes increase the strength of the vane wake and, since there are fewer vanes, it also tends to generate lower frequency excitations on neighboring rotor stages. Because compressor blades, in particular, have highly tapered, long chords with thin leading and trailing edges, they tend to have a number of tip modes with natural frequencies that can be excited by the vane wakes in the operating range of the engine. The workshop participants reported that a characteristic of the resonant response of these high frequency modes is that there tends to be a high degree of variability from blade to blade in the magnitude of the resonant stress. Their experience indicates that only a part of that variation can be attributed to system dynamics and traditional stage mistuning. Following the workshop, a study was initiated to develop a better fundamental understanding of tip mode vibration. This paper documents the results of the first phase of that study.

The objective of the work reported here is to determine the effect of taper and tip thickness on the maximum resonant stress of a tapered beam subjected to externally applied harmonic pressure distributions and to investigate its possible implications to blade vibration. Tapered beams are of interest since their geometry is similar to that of the leading or trailing edge of an airfoil. As a result, airfoil chord-wise bending modes should exhibit similar sensitivity to changes in chord-wise taper and leading or tailing edge thickness. As a result, the tapered beam provides a simplified, first order model of an airfoil's behavior that should provide insight into the sensitivity of the airfoil's response to geometric perturbations.

The sensitivity of the response to geometric changes also depends on the type of excitation that is applied. The spatial distributions of the excitation pressures used in this study are: a constant pressure to serve as a baseline, a leading edge type pressure distribution, and a trailing edge type pressure distribution. Consequently, the relative importance of each type of excitation in terms of how it affects tip mode response will be assessed.

While the free vibration of a tapered beam was originally addressed by Nicholson as early as 1917, and extensive studies were later conducted by Cranch and Adler (1956), Conway and Dubil (1965) and Sanger (1968), the forced response of tapered beams was only recently analyzed by Roy and Ganesan (1992). Roy and Ganesan discuss the amplitude of response of the tapered beam with different thickness profiles that are subjected to a simple sinusoidal harmonic loading. However, they do not investigate the vibratory stresses in the beam, the sensitivity of

Presented at the International Gas Turbine and Aeroengine Congress & Exposition
Houston, Texas - June 5-8, 1995
This paper has been accepted for publication in the Transactions of the ASME
Discussion of it will be accepted at ASME Headquarters until September 30, 1995

the beam to geometric perturbations, or the effect of aerodynamic type pressure fields, which are the focal points of the work reported here.

In the next section, the tapered beam problem will be formulated and a formal solution developed for its resonant response. In section 3, the solution will be specialized for sharply pointed beams, the location and magnitude of the maximum stress will be determined, and the relative importance of the three different types of pressure distributions assessed. In section 4 the effect of blunting the sharp tip will be investigated. The results of the study will be summarized and its possible implications to airfoil resonant response will be discussed in the final section.

2. FORMULATION

The geometry of a beam with a linear height variation is depicted in Figure 1. From Euler-Bernoulli beam theory, the equation of motion is

$$\frac{\partial^2}{\partial x^2}\left(EI(x)\frac{\partial^2 u}{\partial x^2}\right) = -\rho A(x)\frac{\partial^2 u}{\partial t^2} + p(x,t)b \qquad (1)$$

for $t > 0$ and $a < x < L$. $u(x,t)$ is the transverse displacement, E is Young's modulus, b is the width, ρ is the density, and $p(x,t)$ is the pressure. If the height of the beam $h(x)$ is equal to sx, then the section modulus I equals $b(sx)^3/12$ and the area A equals bsx.

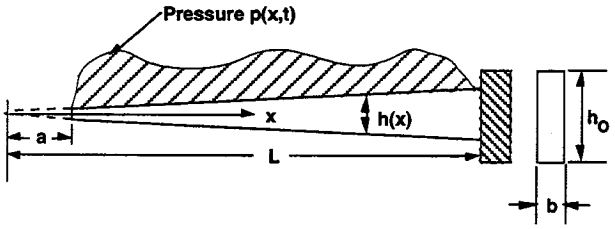

Figure 1: Geometry of a tapered beam

Because of the way the linear height variation has been described, the beam would be sharply pointed if the parameter, a, were zero. Physically, $a \geq 0$ and $\alpha = a/L$ is the *truncation ratio*. The truncation ratio determines the amount of the material removed from the tip and, also, can be used to describe the thickness of the tip.

Using the normalized coordinate $\xi = x/L$, the equation of motion is rewritten as

$$\frac{\partial^2}{\partial \xi^2}\left(\xi^3\frac{\partial^2 u}{\partial \xi^2}\right) = -\gamma^2\xi\frac{\partial^2 u}{\partial t^2} + \tilde{p}(\xi,t) \qquad (2)$$

for $t > 0$ and $\alpha < \xi < 1$, where

$$\gamma^2 = \frac{12\,\rho L^2}{Es^2}$$

and

$$\tilde{p}(\xi,t) = \frac{12\,Lp(\xi,t)}{Es^3}$$

The response of the beam may be represented as a linear combination of its normal modes, i.e.

$$u(\xi,t) = \sum_{i=1}^{\infty} u_n(t)\,\phi_n(\xi) \qquad (3)$$

where, in general, the normal modes are eigenfunctions of the form (Sanger (1968))

$$\phi_n(\xi) = \frac{1}{\lambda_n\sqrt{\xi}}\left[J_1\left(\lambda_n\sqrt{\xi}\right) + B_n Y_1\left(\lambda_n\sqrt{\xi}\right) + C_n I_1\left(\lambda_n\sqrt{\xi}\right) + D_n K_1\left(\lambda_n\sqrt{\xi}\right)\right] \qquad (4)$$

J, Y, I and K are Bessel functions of the first and second kind. The specific values of the constants B_n, C_n, and D_n, and the eigenvalues λ_n depend on α and the boundary conditions. For now, it is assumed that suitable boundary conditions are specified so that the modes are orthogonal.

Substituting (3) into (1) and utilizing orthogonality, a set of uncoupled equations for the modal displacements u_n are obtained of the form

$$\ddot{u}_n(t) + \omega_n^2\,u_n(t) = f_n(t) \qquad (5)$$

where

$$\omega_n^2 = \frac{\lambda_n^4}{16\,\gamma^2}$$

and

$$f_n(t) = \frac{\int_{\alpha}^{1}\tilde{p}(\xi,t)\,\phi_n(\xi)d\xi}{I_n}$$

$$I_n = \int_{\alpha}^{1}\xi\left(\phi_n(\xi)\right)^2 d\xi$$

Incorporating modal damping, the equation of motion is rewritten as

$$\ddot{u}_n(t) + 2\zeta_n\omega_n\dot{u}_n(t) + \omega_n^2 u_n(t) = f_n(t) \qquad (6)$$

If the forcing pressure distribution is harmonic, $\tilde{p}(\xi,t)=\tilde{P}(\xi)e^{i\omega t}$, then the generalized force is given by

$$f_n=\frac{\tilde{P}_n}{\gamma^2 I_n}e^{i\omega t(t)},$$

where

$$\tilde{P}_n=\int_{\alpha}^{1}\tilde{P}(\xi)\phi_n(\xi)d\xi$$

and the steady state response of the beam is

$$u_n(t)=U_n e^{i\omega t} \tag{7}$$

Equations (6) and (7) imply

$$\left(\omega_n^2-\omega^2+2i\omega\omega_n\zeta_n\right)U_n=\frac{\tilde{P}_n}{\gamma^2 I_n} \tag{8}$$

For small values of damping, the resonant response frequency is approximately ω_n and the resonant amplitude of the modal displacement is

$$U_n^*=\left(\frac{1}{2\zeta_n}\right)\frac{1}{\omega_n^2}\frac{\tilde{P}_n}{\gamma^2 I_n} \tag{9}$$

3. RESONANT RESPONSE OF POINTED BEAMS

In this section, the resonant response of pointed beams will be determined in order to serve as a baseline case. The importance of the different types of pressure fields will be established.

3.1 Normal Modes of Vibration

The normal modes of vibration of the tapered pointed cantilever beam can be specialized from (4) and may be written as (Cranch et al. (1956))

$$\phi_n(\xi)=\frac{2}{\lambda_n\sqrt{\xi}}\left[J_1\left(\lambda_n\sqrt{\xi}\right)+C_nI_n\left(\lambda_n\sqrt{\xi}\right)\right] \tag{10}$$

where the mode shapes have been normalized to have unit tip displacement. The natural frequencies are related to the eigenvalues by

$$\omega_n=\frac{\lambda_n^2 h_o}{4L^2}\sqrt{\frac{E}{12\rho}} \tag{11}$$

The modal stresses in the beam can be related to the displacements by

$$\sigma_x=\frac{M_n(\xi)h(\xi)}{I(\xi)}$$

where (12)

$$M_n(\xi)=\frac{EI(\xi)}{L^2}\frac{d^2\phi_n(\xi)}{d\xi^2}$$

Thus, the modal stresses can be written as,

$$\sigma_x(\xi)=\frac{Es\lambda_n^2}{8L}\sigma_n(\xi) \tag{13}$$

where

$$\sigma_n(\xi)=\frac{2}{\lambda_n\sqrt{\xi}}\left[J_3\left(\lambda_n\sqrt{\xi}\right)+C_nI_n\left(\lambda_n\sqrt{\xi}\right)\right]$$

σ_n will be referred to as the *modal stress function.*

The displacements and stress functions of the modes exhibit a strong degree of similarity for the case of the sharply pointed beam. This similarity will be explored in the next section in order to establish a general relationship between the maximum modal stress and the tip displacement of the beam.

3.2 The Maximum Modal Stress and its Location

From (10) and (13) it is clear that the modal displacements and stresses are functions of the variable

$$\chi=\lambda_n\sqrt{\xi} \tag{14}$$

Using χ, the mode shapes and the modal stress function can be rewritten as

$$\phi_n(\chi)=\frac{2}{\chi}\left[J_1(\chi)+C_nI_1(\chi)\right] \tag{15}$$

$$\bar{\phi}_n(\chi)=\frac{2}{\chi}\left[J_3(\chi)+C_nI_3(\chi)\right] \tag{16}$$

The first seven modal displacements and modal stress functions are plotted as a function of χ in Figures 2 and 3. In these figures the functions are only displayed over physically meaningful values of χ. When plotted in this manner it is apparent that in the near field, χ small, all modes behave in a similar fashion. This occurs because only the coefficient C_n varies with the mode

number n in expressions (15) and (16), and it plays a limited role in the functions' near field behavior. From Figure 3 it is clear that the maximum value of the modal stress function, σ^o, is approximately equal to 0.22 for all modes, but, especially for the higher (n > 1) modes. Let $(\sigma_n)_{max}$ be the maximum value of the modal stress when the beam resonates in the n^{th} mode. From equation (13) it can be related to the resonant displacement of the beam as

$$(\sigma_n)_{max} = \frac{Es\,\lambda_n^2}{8\,L}\sigma^o\,U_n^* \qquad (17)$$

or alternatively using (2) and (5) as

$$(\sigma_n)_{max} = 0.38\,U_n^*\,\omega_n\sqrt{\rho E} \qquad (18)$$

This is similar to Ungar's result (1962) for simply supported, uniform beams, i.e., he found that $(\sigma_n)_{max} = U_n^*\omega_n\sqrt{3\rho E}$. However, for the case of tapered beams the ratio of stress to maximum displacement is smaller since the tip is considerably more flexible.

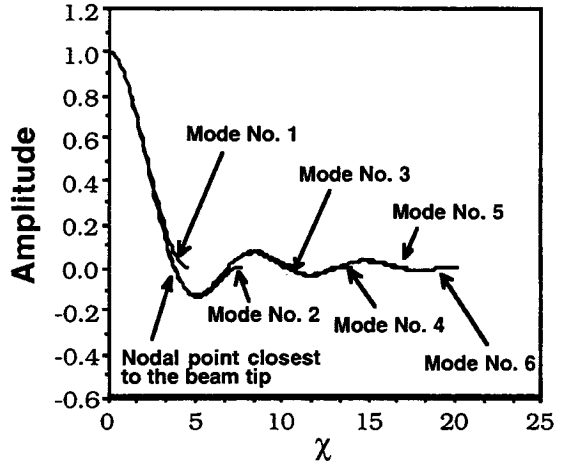

Figure 2: Mode shapes for the cantilever beam

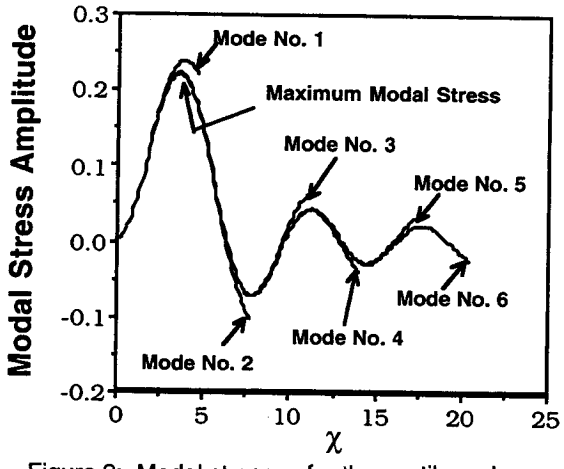

Figure 3: Modal stresses for the cantilever beam

From Figures 2 and 3, it can be observed that the distance to the first nodal point and the distance to the maximum stress location is nearly the same for all modes but especially for n > 1. In fact, it can be shown numerically that the maximum stress occurs at a value of χ equal to approximately 0.95 of the distance to the first nodal point. Since χ is proportional to $\sqrt{\xi}$ this physically means that the maximum modal stress occurs at a distance from the tip of the beam which is approximately 89% of the distance to the first nodal point.

The magnitude and location of the maximum stress were calculated when other boundary conditions were applied at $\xi = 1$. Each case exhibited results for the higher modes that were essentially the same as those discussed in this section. Consequently, it can be concluded that the maximum stresses in all but the lowest modes are approximately given by (17) or (18), and, in fact, is to a great extent independent of the constraints applied away from the tip.

3.3 Maximum Resonant Stress

From equations (9) and (17), the maximum resonant stress in the tapered beam is given by

$$(\sigma_m)_{peak} = \frac{24}{s^2}\left(\frac{1}{2\zeta_m}\right)\delta_m \qquad (19)$$

where the expression has been simplified to

$$\delta_m = \frac{\sigma^o\,P_m}{\lambda_m^2\,I_m} \quad \text{and} \quad P_m = \int_0^1 P(\xi)\phi_m(\xi)d\xi \qquad (20)$$

and where $P(\xi)$ is the original, physical pressure distribution. From (19) it can be observed that the resonant stresses depend on three factors. Firstly, they are directly proportional to the dynamic amplification factor, $1/(2\zeta_m)$. This dependence will not be investigated in this study. Secondly, they are inversely proportional to the square of the slope ($s = h_o/L$) and for small values of s, the stresses are very sensitive to variations in h_o, the thickness at the root of the beam. Lastly, they are proportional to δ_m, the *stress participation factor*. The stress participation factor directly evaluates the influence of the type of pressure distribution on the resonant stress. This dependence will be explored in the next section.

3.4 Calculation of Stress Participation Factors

The stress participation factors are determined for the three types of pressure distributions defined as (E. H. Dowell (1989))

$$\begin{aligned} &\text{Baseline Case of Constant Pressure:} && p(\xi,t) = p_o\,e^{i\omega t} \\ &\text{Leading Edge Type Pressure:} && p(\xi,t) = \frac{P_1}{\sqrt{\xi}}\,e^{i\omega t} \\ &\text{Trailing Edge Type Pressure:} && p(\xi,t) = P_2\sqrt{\xi}\,e^{i\omega t} \end{aligned} \qquad (21)$$

In each case, the constants, P_i, are chosen so that the average pressure distribution acting on the beam is equal to one.

The participation factors were computed for each type of pressure distribution and the results plotted as a function of mode number in Figure 4. (The points are connected artificially by lines to better identify the type of pressure distribution applied.)

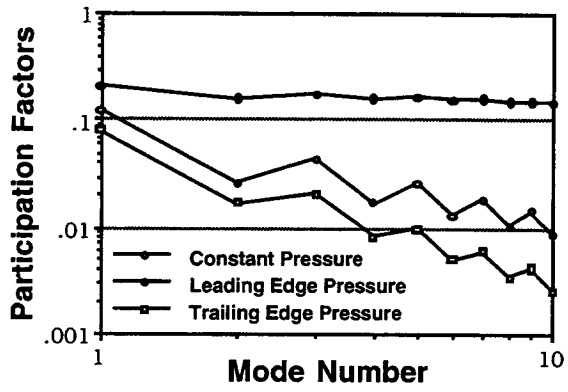

Figure 4: Stress participation factors

For the case of constant pressure, the odd modes show a higher participation than the even modes. Consequently, for this type of pressure distribution, the odd modes would tend to be more critical than the even numbered ones.

For a trailing edge type pressure distribution, the participation factors for odd modes were again more critical than those for the even number modes. However, the blades tended to respond considerably less than if a constant pressure were applied with the same average value. This occurs because the applied pressures are smaller near the tip where the displacement is highest and, consequently, the generalized force is smaller. Since for the higher frequency modes the displacements tend to be progressively more localized near the tip, the generalized force decreases as the mode number increases and the participation factors decrease accordingly. From a vibratory response point of view, trailing edge type pressure fields provide the least critical source of excitation.

For a leading edge type of pressure distribution the participation factors of the higher modes were of the same magnitude as that of the first mode. This could be expected since this type of distribution produces a singularity at the free tip of the beam which is similar in effect to the application of a delta function at the beam tip. Delta functions tend to excite all modes equally, which is nearly true in this case. This is a matter of serious concern as it implies that the peak vibratory stresses due to higher modes could be quite large.

From a resonant response point of view, the critical case is a thin leading edge with pressure distributions that are highly localized at the tip. According to the previous analyses all modes, including the higher frequency ones, may be excited to the nearly same degree. In theory for a perfectly pointed beam, the location of the maximum stress occurs closer to the tip as the mode number increases. In fact, however, airfoils are not perfectly pointed as their tips are cut-off and slightly rounded. By truncating the sharp tips in this manner, the higher frequency modes may be preferentially affected. This effect is investigated in the next section.

4. RESONANT RESPONSE OF TRUNCATED BEAMS

In this section, the effect of removing a portion of the sharp tip is investigated. Truncating the beam in this manner will be shown to be equivalent to increasing the tip's thickness.

4.1 Normal Modes of Vibration

The normal modes of vibration of a tapered truncated cantilever beam are

$$\phi(\xi)=\frac{1}{\phi_n^o}\frac{1}{\lambda_n\sqrt{\xi}}\Big[J_1\left(\lambda_n\sqrt{\xi}\right)+B_nY_1\left(\lambda_n\sqrt{\xi}\right)+C_nI_1\left(\lambda_n\sqrt{\xi}\right)+D_nK_1\left(\lambda_n\sqrt{\xi}\right)\Big] \tag{22}$$

where $\alpha < \xi < 1$ and

$$\phi_n^o=\frac{1}{\lambda_n\sqrt{\alpha}}\Big[J_1\left(\lambda_n\sqrt{\alpha}\right)+B_nY_1\left(\lambda_n\sqrt{\alpha}\right)+C_nI_1\left(\lambda_n\sqrt{\alpha}\right)+D_nK_1\left(\lambda_n\sqrt{\alpha}\right)\Big]$$

where the purpose of ϕ_n^o is to normalize the modes so that they have unit tip displacement. Analogous to equation (13) the modal stresses are again of the form

$$\sigma_x(\xi)=\frac{Es\,\lambda_n^2}{8L}\sigma_n(\xi) \tag{23}$$

except that the modal stress function is given by

$$\sigma_n(\xi)=\frac{1}{\phi_n^o}\frac{1}{\lambda_n\sqrt{\xi}}\Big[J_3\left(\lambda_n\sqrt{\xi}\right)+B_nY_3\left(\lambda_n\sqrt{\xi}\right)+C_nI_3\left(\lambda_n\sqrt{\xi}\right)+D_nK_3\left(\lambda_n\sqrt{\xi}\right)\Big]$$

4.2 Scaling of Mode Shapes and the Modal Stress Function

The location and the magnitude of the maximum modal stress is now more difficult to determine since an additional parameter α has been introduced. In section 3.2, it was observed that the location of the maximum stress for a mode depended on the location of the first nodal point. Let ξ_ϕ be the distance to the

first nodal point of a mode, ξ_σ be the distance to the point where the modal stress is a maximum, and $\mu = \xi_\sigma/\xi_\phi$. Define the maximum value of $\sigma_n(\xi)$ for $\alpha < \xi < 1$ as σ^α. After some investigation, it was found that the μ and σ^α could best be described in terms of the *truncation factor*, κ, which combines two parameters. The truncation factor is defined as

$$\kappa(\alpha) = \frac{\alpha}{\xi_\phi(\alpha) - \alpha} \tag{24}$$

μ and σ^α were calculated for a series of cantilevered beams and plotted as functions of κ for the first seven modes in Figure 5. With the exception of the first mode, μ and σ^α are essentially the same for all modes. The different behavior of the first mode is probably due to the fact that the constraints at its first nodal point are different from those of the interior nodal points associated with the higher modes.

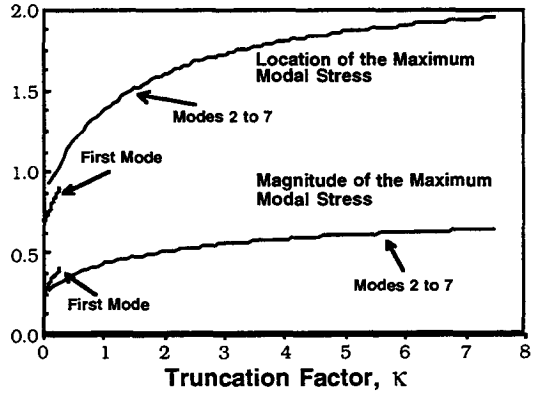

Figure 5: Location and magnitude of the maximum modal stress

Thus, if the tip displacement in the n^{th} mode U_n^* is known, then analogous to (17) the maximum stress in the beam is given by

$$\left(\sigma_n(\alpha)\right)_{max} = \frac{Es\,\lambda_n^2}{8\,L}\sigma^\alpha U_n^* \tag{25}$$

4.3 Maximum Resonant Stress

Analogous to section 3.3, the maximum resonant stress for truncated beams is given by

$$\left(\sigma_n\right)_{peak} = \frac{24}{s^2}\left(\frac{1}{2\zeta_n}\right)\delta_n(\alpha) \tag{26}$$

where

$$\delta_n(\alpha) = \frac{\sigma^\alpha\, P_n}{\lambda_n^2\, I_n} \tag{27}$$

The stress participation factor, $\delta_n(\alpha)$ depends on the type of pressure loading and the truncation ratio, α. It was found in section 3.4 that a leading edge pressure distribution most strongly excited the critical high frequency modes. $\delta_n(\alpha)$ was calculated for this critical case for the first seven modes. In these calculations the pressure remained singular at the beam tip, i.e., $P(\xi) = P_1/\sqrt{\xi - \alpha}$, and P_1 was set equal to $0.5/\sqrt{1-\alpha}$ so that the net force remained constant. The results are depicted in Figure 6 in which $\delta_n(\alpha)$ is plotted as a function of the mode number for α varying from 0 to 10%. It shows that in the range of values simulated, increasing α uniformly caused $\delta_n(\alpha)$ to decrease. Furthermore, the decrease is more rapid when the mode number is higher.

The information in Figure 6 is consolidated when $\delta_n(\alpha)/\delta_n(0)$ are plotted as functions of the truncation factor κ as shown in Figure 7. Figure 7 provides a fairly general result. For example, it indicates that, except for the first mode, removing material from the tip so that κ equals 10% will reduce the resonant vibratory stress by 80%.

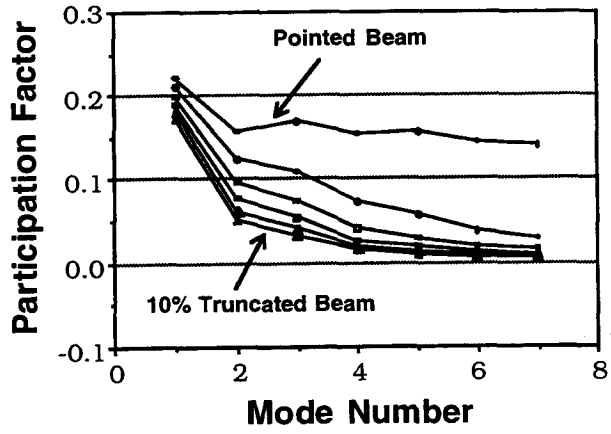

Figure 6: Effect of truncation on stress participation factors

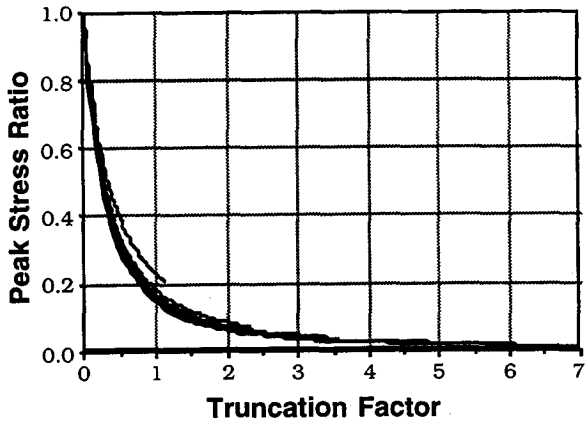

Figure 7: Reduction in stress participation factor

An alternative physical interpretation of these results is to consider the effect of keeping the length of the beam and its base thickness fixed and thickening its tip. If h_t and h_o are the thicknesses of the beam at its tip and base, respectively, then $\alpha = h_t/h_o$. Thus, Figures 6 and 7 also effectively describe the effect of changing the beam's tip thickness on the stress participation factor. Note that, in this case, the slope s decreases as α increases since $s = h_o(1 - \alpha)/L$ and that from (26) this will have some effect on the magnitude of the resonant stress.

While the results indicated in Figure 7 are quite general, they are not in the best form for use by engineers. An alternative way of viewing this data would be to pose the question, "What thickness ratio is required to reduce the resonant stress by a certain percent?" For example, the thickness ratio, h_t/h_o, that is required to reduce the resonant stress by 50% is plotted as a function of the mode number in Figure 8. The least squares fit of the data, indicated in Figure 8 as a solid straight line, yields the result that to reduce the resonant stress in the n^{th} mode by at least 50% the thickness ratio should satisfy

$$\frac{h_t}{h_o} \geq \left(\frac{5}{n}\right)^{1.85} \tag{28}$$

It is clear from (28) that the response of the higher frequency modes is very sensitive to small changes in the thickness of the tip.

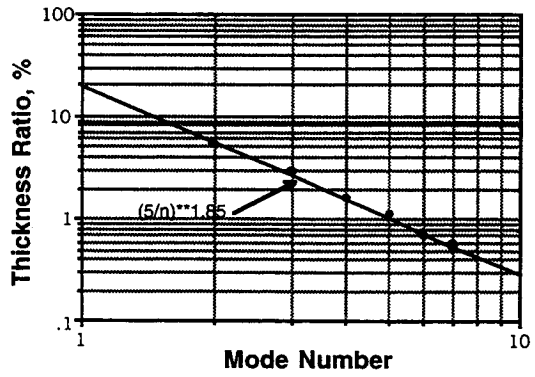

Figure 8: Tip thickness required to reduce stress by a factor of two

5. CONCLUSIONS

A study of the resonant stress that occurs in linearly tapered beams was conducted in which the beams were subjected to three different types of loading. The load distributions were chosen to represent the type of pressure fields that occur on the leading and trailing edges of airfoils as well as a baseline constant pressure case. These cases were investigated because the beam's response should provide a first order model of the behavior of high frequency, chord-wise bending modes in airfoils.

Expressions were derived using a normal mode expansion for the beam's resonant displacement. In order to relate the displacement to stress, the modal stress function was examined to determine the magnitude and location of the maximum stress in the beam. For the case of a sharply pointed beam, the magnitude of the maximum stress was found to be approximately $0.38\,\omega_n\sqrt{\rho E}$ times the tip displacement and it occurs at a location that is approximately 89% of the distance to the first nodal point. In the case of a truncated beam, the magnitude and location of the maximum stress were found to be functions of a single parameter, the truncation factor, κ.

Using these results, expressions were derived for the maximum resonant stress under the assumption that the modal damping factors either remain constant or can be independently calculated. The resonant stress of the n^{th} mode was found to be inversely proportional to the square of the taper parameter, s, and proportional to a stress participation factor, δ_n. The stress participation factor was calculated for sharply pointed beams for three types of pressure distributions. It was found to decrease fairly rapidly for the higher modes except for the critical case of a leading edge type pressure distribution. For this case, δ_n was nearly constant as n increased. This suggests that an important source of excitation for chord-wise bending modes in airfoils may be the pressure fields near their leading edge.

A practical method for reducing tip mode response that is used by airfoil designers is to blunt the sharp edge by either thickening or removing part of its tip. It was found that both treatments are essentially equivalent and that they are predicted to significantly reduce the resonant response of the tapered beam in the case of a leading edge-type pressure distribution. It was shown that the response of all of the higher frequency modes were similarly reduced if the participation factors were plotted as a function of the truncation factor, κ. Results that were not shown indicated that similar blunting of the beam when it is subjected to a trailing edge type pressure distribution could lead to an increase in vibratory response. Thus, the type of pressure loading should be taken into account when trying to remedy a resonant response problem by changing an airfoil's geometry.

A goal of this work was to obtain a more basic understanding of chord-wise bending modes in airfoils, and, in particular, to establish possible sources of the large variability that has been observed in their resonant response. A key result in this regard may be the consolidated plot of the normalized stress participation factor as a function of the truncation factor, κ, as displayed in Figure 7. Because the participation factor varies rapidly when κ is small, it is clear that the response of a specific high frequency mode would be highly sensitive to variations in the tip's thickness if its nominal thickness corresponded to a κ value in this range, e.g., $\kappa_{nom} = 0.2$. Typically, for any given design, there will be one or possibly a group of neighboring modes that satisfy this requirement and exhibit corresponding increased sensitivity to thickness variations.

Because of the simplified nature of the model, it is clear that this study is preliminary in nature. Two issues that bear on its accuracy are how well Euler-Bernoulli beam theory represents tapered beams and, to what extent the behavior of tapered beam modes represent actual blades. A significant number of independent calculations were performed on tapered beam geometries using a commercial finite element program in order to check the accuracy of the results. The tapered beam geometry was represented using a relatively fine mesh of two dimensional, quadrilateral elements. It was observed that for the modes discussed in this paper, the participation factors that were calculated using finite elements agreed reasonably well with those predicted by Euler-Bernoulli beam theory and that, as a result, all of the trends were the same as those presented in this paper. Thus, it was concluded that Euler-Bernoulli theory provides a reasonably accurate representation of the modes and beam geometries of interest and, of course, has the advantage of providing much more general results than can be obtained from numerical simulations.

A more serious concern is to what extent the behavior of tapered beams represents that of blades. This issue is complex and remains to be studied. However, it is important to understand that the purpose of a simple model, such as that presented here, is to provide insights into some of the physical mechanisms that should also be factors affecting the behavior of the more complex, real system. In this sense the simple model provides a context for the subsequent study of the actual system.

ACKNOWLEDGEMENTS

This work was supported by the GUIde Consortium on the Forced Response of Bladed Disks. Support for the Consortium is provided by its industrial members: AlliedSignal Engines, Allison Engine Company, General Electric Aircraft Engines, Pratt & Whitney, Textron Lycoming, Westinghouse Electric Corporation, NASA, and the U.S. Air Force. Special acknowledgment is given to the members of the Steering Committee for their suggestions and practical knowledge of the problem discussed.

REFERENCES

Conway, H. D. and Dubil, J. F., 1965, "Vibration frequencies of truncated-cone and wedge beams," *Journal of Applied Mechanics., Trans. ASME*, Vol. 87, pp. 932-934.

Cranch, E. T. and Adler, A. A., 1956, "Bending vibrations of variable section beams," *Journal of Applied Mechanics, Trans. ASME*, Vol. 78, pp. 103-108.

Dowell, E. H., Curtiss, H. C., Scanlan, R. H., and Sisto, F., 1989, *A modern course in aeroelasticity*, Kluwer Academic Publishers, Boston, second edition.

Nicholson, J. W., 1917, "The lateral vibrations of bars of variable section," *Proceedings of the Royal Society of London, England*, Vol. 93, Series A, pp. 506-519.

Roy, P. K. and Ganesan, N., 1992, "Some studies on the response of a tapered beam," *Computers and Structures*, Vol. 45, No. 1, pp. 185-195.

Sanger, D. J., 1968, "Transverse vibration of a class of non-uniform beams," *Journal Mechanical Engineering Science*, Vol. 10, No. 2, pp. 111-120.

Ungar, Eric E., 1962, "Maximum stresses in beams and plates vibrating at resonance," *Journal of Engineering for Industry*, Vol. 84, pp. 149-155.